Integrated Environmental Assessment and Management — Volume 18, Number 4—pp. 909–920
Received: 15 April 2021 | Returned for Revision: 19 May 2021 | Accepted: 11 July 2021

Special Series

Novel approach to large-scale monitoring of submerged aquatic vegetation: A nationwide example from Sweden

Silvia Huber,[1] Lars B. Hansen,[1] Lisbeth T. Nielsen,[1] Mikkel L. Rasmussen,[1] Jonas Sølvsteen,[1] Johnny Berglund,[2] Carlos Paz von Friesen,[2] Magnus Danbolt,[3] Mats Envall,[4] Eduardo Infantes,[4] and Per Moksnes[4]

[1]*DHI GRAS A/S, Hørsholm, Denmark*
[2]*Länsstyrelsen Västerbotten, Umeå, Sweden*
[3]*Länsstyrelsen Kalmar, Kalmar, Sweden*
[4]*Department of Marine Sciences, University of Gothenburg, Gothenburg, Sweden*

EDITOR'S NOTE:

This article is part of the special series, "The Future of Marine Environmental Monitoring and Assessment." The series takes a sneak peek into the future of marine monitoring, where integrating new monitoring technologies with advanced ecosystem modeling will make it possible to estimate real-time ecosystem status, improve model precision, and provide a robust basis for marine environmental assessments.

Abstract

According to the EU Habitats directive, the Water Framework Directive, and the Marine Strategy Framework Directive, member states are required to map, monitor, and evaluate changes in quality and areal distribution of different marine habitats and biotopes to protect the marine environment more effectively. Submerged aquatic vegetation (SAV) is a key indicator of the ecological status of coastal ecosystems and is therefore widely used in reporting related to these directives. Environmental monitoring of the areal distribution of SAV is lacking in Sweden due to the challenges of large-scale monitoring using traditional small-scale methods. To address this gap, in 2020, we embarked on a project to combine Copernicus Sentinel-2 satellite imagery, novel machine learning (ML) techniques, and advanced data processing in a cloud-based web application that enables users to create up-to-date SAV classifications. At the same time, the approach was used to derive the first high-resolution SAV map for the entire coastline of Sweden, where an area of 1550 km^2 was mapped as SAV. Quantitative evaluation of the accuracy of the classification using independent field data from three different regions along the Swedish coast demonstrated relative high accuracy within shallower areas, particularly where water transparency was high (average total accuracy per region 0.60–0.77). However, the classification missed large proportions of vegetation growing in deeper water (on average 31%–50%) and performed poorly in areas with fragmented or mixed vegetation and poor water quality, challenges that should be addressed in the development of the mapping methods towards integration into monitoring frameworks such as the EU directives. In this article, we present the results of the first satellite-derived SAV classification for the entire Swedish coast and show the implementation of a cloud-based SAV mapping application (prototype) developed within the frame of the project. *Integr Environ Assess Manag* 2022;18:909–920. © 2021 The Authors. *Integrated Environmental Assessment and Management* published by Wiley Periodicals LLC on behalf of Society of Environmental Toxicology & Chemistry (SETAC).

KEYWORDS: Ecological status, Environmental monitoring, Machine learning, Sentinel-2

INTRODUCTION

Coastal waters are highly productive and diverse ecosystems, particularly if dominated by belts of submerged aquatic vegetation (SAV). Submerged aquatic vegetation includes a taxonomically diverse group of macroalgae and seagrasses that lives below the water surface in coastal and estuarine waters and grows as large meadows, sometimes in smaller patches. The presence, type, and abundance of aquatic vegetation are key indicators of the ecological status and environmental state of ocean and estuarine waters (Marbà et al., 2013). Aquatic vegetation, seagrass in particular, provides critical ecosystem functions and services to humans; such functions and services are difficult to replace and include: habitats and spawning grounds for many

Correspondence Silvia Huber, DHI GRAS A/S, Hørsholm, Denmark.
Email: shu@dhigroup.com

Published 16 July 2021 on wileyonlinelibrary.com/journal/ieam.

This is an open access article under the terms of the Creative Commons Attribution-NonCommercial-NoDerivs License, which permits use and distribution in any medium, provided the original work is properly cited, the use is non-commercial and no modifications or adaptations are made.

different marine species; uptake and long-term storage of CO_2 and nutrients that mitigate climate change and reduce eutrophication, respectively; reduction in wave energy and stabilization of the sediment, which reduce sediment resuspension and erosion; and improvement of water quality (Barbier et al., 2011; Cole & Moksnes, 2016; Infantes et al., 2012; Moksnes et al., 2021). Due to the nature of their important ecosystem functions, up-to-date knowledge of SAV abundance and growth dynamics is critical to assess the impacts of management and conservation efforts and monitor overall marine health (J. E. Duffy et al., 2019; Frigstad et al., 2021; United Nations Environment Programme, 2020).

In the European Union, monitoring and assessment of the status of marine waters are key components of the Water Framework Directive (WFD), the Marine Strategy Framework Directive (MSFD), and the Habitats Directive (HD). While the WFD and MSFD use the terms Good Ecological Status and Good Environmental Status, respectively, the HD assesses and reports on "Favourable Conservation Status" (FCS). All directives require reporting every sixth year. Overall, these directives consider SAV in one form or another, each with a somewhat different purpose, yet all with the goal of protecting the marine environment across Europe more effectively.

To assess FCS for habitats, biogeographical information about range, area, and structure and function (often referred to as quality) of the habitats is needed (DG Environment, 2017). Habitat types are considered in an FCS when the natural range of the habitat type is stable or increasing, long-term survival of specific structure and functions is considered secure, and the status of its typical species is favorable (Council Directive 92/43/EEC). Changes in spatial coverage or density of SAV reflect the structure and function of shallow marine habitats, such as: sublittoral sandbanks, estuaries, mudflats, and lagoons (Torn et al., 2017). In the WFD, the depth distribution of SAV is regularly used as an indicator of good ecological status. If the water gets enriched with nutrients, transparency decreases, less light penetrates into the water column and, consequently, the depth distribution of SAV decreases (Kuuppo et al., 2006; Nielsen et al., 2002). In the MSFD, SAV is used as an important biological indicator to assess the status of two separate quality descriptors: biodiversity and eutrophication (Ferreira et al., 2011).

In Sweden, environmental monitoring of the areal distribution of SAV is lacking, as in many other European countries (European Commission, 2017; Moksnes et al., 2016; SWAM, 2014). So far, national monitoring of macrophytes in Sweden has focused on depth distribution and has been carried out mainly on hard substrates. This lack of information about the areal distribution of SAV growing on soft bottom substrates was identified as an inadequacy during the initial assessment of coastal vegetation in Sweden for the MSFD (SWAM, 2012) and a clear obstacle impeding the effectiveness of the WFD in the protection of eelgrass habitats (Moksnes et al., 2016). Information on the areal distribution of eelgrass and other marine habitats is also required for the assessment of FCS under the EU Habitat Directive, for monitoring Natura 2000 sites, and other measures (Dahlgren et al., 2012).

Most common SAV monitoring methods involve field-based observations, for instance, through diving, optical methods based on aerial and underwater drones, aerial photographs or commercial very high-resolution satellite imagery, and acoustic technologies such as single-beam echosounding sidescan and multibeam sonars. These methods all provide highly detailed information on coverage and distribution of SAV, but also have certain limitations. They either cover only smaller areas, and are therefore not suitable for large-scale assessments, or the data collection is expensive and unsystematic, thus hindering consistent, repeatable mapping of SAV. This limits our ability to comprehensively capture the distribution and dynamics of these underwater coastal communities and how they change through time. (J. E. Duffy et al., 2019; Rowan & Kalacska, 2021; Stæhr et al., 2019; Timmermann et al., 2021). However, all of these technologies are widely used and needed to validate satellite-based technologies.

At large scale, analyzing free satellite remote-sensing imagery is the only cost-efficient method that can facilitate operational and consistent monitoring of SAV. All year and systematic satellite sensors can cover large areas quickly and repeatedly, allowing the assessment of different vegetation stages during the growing season in optically shallow waters that are sufficiently clear. However, like all optical methods, the satellite-based approach reaches its limits in deeper and/or turbid waters. In these so called "optically deep waters," the incoming light does not reach the seabed and thus, the benthos cannot be detected by satellites. Detecting SAV distribution down to the depth limit is therefore often challenging using optical methods.

To respond to the information gap in Sweden, this project was initiated with three primary objectives: (1) produce the first nationwide marine-habitat map at 10 m spatial resolution with the description of three classes: SAV, soft substrate without vegetation, and hard substrate without vegetation, using Copernicus S2 satellite imagery captured between 2019 and 2020; (2) develop a cloud-based SAV classification application (prototype) based on machine learning (ML) and S2 imagery to be operated by officers with different levels of experience; (3) evaluate the accuracy in the SAV classification estimated using S2 imagery with survey and aerial drone data.

The results of the project are used to determine if large-scale, S2-based SAV classifications can be considered for future monitoring obligations, and if it would make sense to pursue the development of a fully functional SAV mapping application based on the results of the prototype.

MATERIALS AND METHODS

Study area

The project included the entire shallow coastal zone of Sweden, an area covering almost 50 000 km^2. The estimated

 © 2021 The Authors

FIGURE 1 Area of interest along the shallow Swedish coast. The nationwide submerged aquatic vegetation map was produced for all of the regions shown in this overview, and the cloud-based application allows mapping of these coastal regions. Before the analysis, the shallow coastal zone of Sweden was divided into 54 regions, mainly for reasons of data handling. Red numbers denote areas where independent ground-truth data were collected along the Swedish NW coast (1), in Kalmar Sound along the SE coast (2), and in the Bothnian Bay along the Swedish NE coast (3) using drop video and drone images

total area that is shallower than 10 m covers 9300 km^2 according to nautical chart data (Naturvårdsverket, 2006). Before the analysis, the coastline was divided into 54 regions considering environmental characteristics (i.e., water quality) and Sentinel-2 scene edge effects, mainly for better handling of the classification model (Figure 1). The Swedish coastline represents major gradients in environmental conditions in terms of salinity, eutrophication, seabed substrate, temperature, and exposure, at both small and large scales (Wikström et al., 2016).

Input satellite data

We used imagery from the Copernicus S2 mission, which comes in the constellation of two satellites (S2A and S2B) in a sun-synchronous orbit. Sentinel-2A was launched in June 2015 and S2B in July 2016. The data are free of charge and globally available, with a revisit time of every 5 days at the equator and every 2–3 days in Sweden. Each of the satellites hosts a Multi-Spectral Instrument covering 13 spectral bands spanning from the visible to the shortwave infrared (443–2190 nm), with a swath width of 290 km (TAS, 2021).

For the SAV mapping, the first four optical bands of S2 (coastal aerosol, blue, green, and red) were used, all of which have a spatial resolution of 10 × 10 m, with the exception of the coastal aerosol band, which has a spatial resolution of 60 m. Therefore, the coastal aerosol band was resampled to 10 m to match the other input bands and achieve a high resolution in the SAV map. To cover the entire Swedish coastline, 35 S2 tiles are required. Each tile covers 100 × 100 km and is approximately 600 MB in size. We selected images mainly from spring and summer 2019. For seven regions out of 54, data from April to June 2020 was used because no suitable dataset from 2019 was available. The images used for further processing and eventually mapping were selected based on criteria such as cloud cover and haze, available sunlight, and water transparency.

Satellite data preprocessing

Before classification, the satellite imagery needs to be preprocessed to remove atmospheric and other surface effects. Atmospheric correction was performed with Sen2Cor processor v2.8 (Main-Knorn et al., 2017). Sen2Cor performs the atmospheric, terrain, and cirrus correction of S2 Level-1C Top-Of-Atmosphere to derive a Level-2A Bottom-Of-Atmosphere reflectance product. The cloud and/or shadow layers produced by Sen2Cor for each image were used to mask out clouds and their shadows. Shadows on water are difficult to map and Sen2Cor's overall cloud and/or shadow layer accuracy has been recently reported to be 84% (Baetens et al., 2019), that is, some minor artifacts related to clouds or shadows could still be present in the classification.

Sun glint was removed with the method described in Lee et al. (1999). Sun glint is a serious confounding factor for the mapping of benthic features because the component of the satellite-received signal from the water surface can be much greater than the signal relative to subsurface features.

Auxiliary input layers

The core input data for the SAV classification are the water subsurface reflectance from preprocessed S2 imagery. However, to increase classification model robustness, generality, and transferability in space and time, several auxiliary datasets have been derived to be used together with the reflectance data to train the ML model and predict SAV. The following auxiliary layers were derived:

(a) Satellite-derived bathymetry (SDB) at 10 m spatial resolution from best available S2 imagery from 2018 to 2020 for the entire Swedish shallow coast (<10 m depth).
(b) Feasibility layer derived from best available S2 imagery from 2018 to 2020 with four classes: (1) land, (2) optically deep water, (3) optically shallow water with good visibility (covering 2560 km^2), and (4) optically shallow water with potentially good visibility (covering 1300 km^2). The feasibility layer is a byproduct of the SDB retrieval and basically describes where SDB retrieval was successful (optically shallow areas) and where it failed (land and optically deep waters). The depth limits of shallow

waters vary, depending on the quality of the S2 input imagery and the water quality during satellite image acquisition. Therefore, we produced two shallow water classes. The class *shallow water with good visibility* describes all areas where we had exceptionally good visibility in the imagery used for producing the SDB; the class *optically shallow water with potentially good visibility* indicates areas where we found the bathymetric retrievals to be uncertain with the available imagery, mainly owing to environmental conditions, but for which better imagery might become available in future. Hence the feasibility layer depends strongly on the S2 input imagery.

(c) Depth-invariant indices (water column correction) based on S2 reflectance to remove the influence of depth (attenuation) from spectral data indices (Stumpf et al., 2003).

(d) Convolutions (filters) calculated from S2 subsurface reflectance to include the geospatial context with different window sizes (50–500 m).

SAV mapping

Machine learning. The backbone of the SAV mapping method is a light gradient boosting machine (LGBM; Ke et al., 2017), which is a freely distributed, open source gradient boosting framework for ML originally developed by Microsoft. The LGBM was chosen because it is a powerful and efficient technique for building predictive models; the training process is fast, additional training polygons can be added easily at any stage, and the model can be applied to very large datasets.

Training data collection. The key to achieving good results with any ML algorithm is the quality and amount of sample data (training data) used to train the model to make predictions. We used more than 30 000 labeled polygons and points, containing representative characteristics of the three habitat classes (a) SAV, (b) unvegetated soft substrate (sand), and (c) unvegetated hard substrate (rocks) distributed along the entire shallow Swedish coast. Experienced satellite remote-sensing experts delineated the training samples, based on photointerpretation, with the help of flight orthophotos. In areas with relatively high water clarity, dense eelgrass meadows, and a clear contrast between SAV and the underlying substrate, it was easier to extract good training samples than in waters with high turbidity and more patchy SAV growth. More than 16 000 polygons were extracted for SAV (~244 km^2), 12 000 for sand (~324 km^2), and 8000 for the rock habitat types (~122 km^2). For each region, a separate model was trained; that is, we had 54 different predictive models. The trained LGBM models achieved a classification accuracy of approximately 97% on a test dataset, which contained randomly selected 10% of the training dataset that was set aside for accuracy testing at the beginning and not used in the training of the ML model.

Trained predictive models were applied to all preselected S2 images. After the SAV mapping was conducted for all 54 regions, sieving was run on the habitat classifications to remove all objects smaller than 8 pixels. In addition, all maps were checked for artifacts at region borders and, if needed, the respective LGBM model was updated and rerun to derive a coherent SAV map for Sweden.

Quantitative evaluation of the SAV map. In 2019, ground-truth data were collected from 10 shallow soft substrate sites along the northwest (NW) Swedish coast to assess the accuracy of classifications based on 2019 satellite images and the relative SAV areal distribution. A standard GPS (Garmin GPSmap64) with relatively low precision (±3–4 m) was used for the data collection. Because these data were not ideal to assess the accuracy of satellite image classification, we carried out a second set of accuracy estimates using ca. 200–400 random points generated from drone classifications as ground-truth data. To obtain estimates from the Swedish east coast (Baltic Sea), we carried out new satellite image classification of selected areas in 2020, which were evaluated with ground-truth data collected the same year and month. The datapoints were collected at random using RTK-GPS (Trimble Geo7X) with a precision of ±20 cm. Only field data were used to estimate the satellite classification accuracy for this area. In Kalmar Sound, along the Swedish SE coast, four shallow soft substrate sites were assessed; in the Bothnian Bay along the Swedish NE coast, one site was tested (Figure 1). At all sites, we also classified SAV and unvegetated soft substrates using high-resolution drone images for comparison. At each site, ca. 50–100 ground-truth data points were collected using drop video with a life view (SeaViewer) or an aquascope from the shallowest part of the bays to the maximum depth distribution of the vegetation. Dominating vegetation and substrate were visually estimated within an area of approximately 1–5 m^2. Drone images were collected with a commercial drone with a digital RGB camera (DJI Phantom 4 Pro) and converted into georeferenced ortho mosaics where SAV and unvegetated soft substrates were classified using GIS software (ArcGIS Pro; e.g., J. P. Duffy et al., 2018; Husson et al., 2016).

The accuracy of the satellite images was assessed within the shallow area at each site identified by the feasibility layer of the analyses, and a confusion (error) matrix of accuracy was estimated using the ground-truth data (e.g., Olofsson et al., 2014). Based on the confusion matrix, the producer, the user, and total accuracies are estimated. The first demonstrates for each class the probability that a randomly chosen point in field has the same class value on the map. The user accuracy demonstrates the probability that a randomly chosen point on the map has the same class value in the field, and the total accuracy is computed by dividing the total number of correctly classified pixels by the total number of reference pixels.

To assess the precision of SAV areal estimates from satellite classifications, we used the drone classified SAV as

 © 2021 The Authors

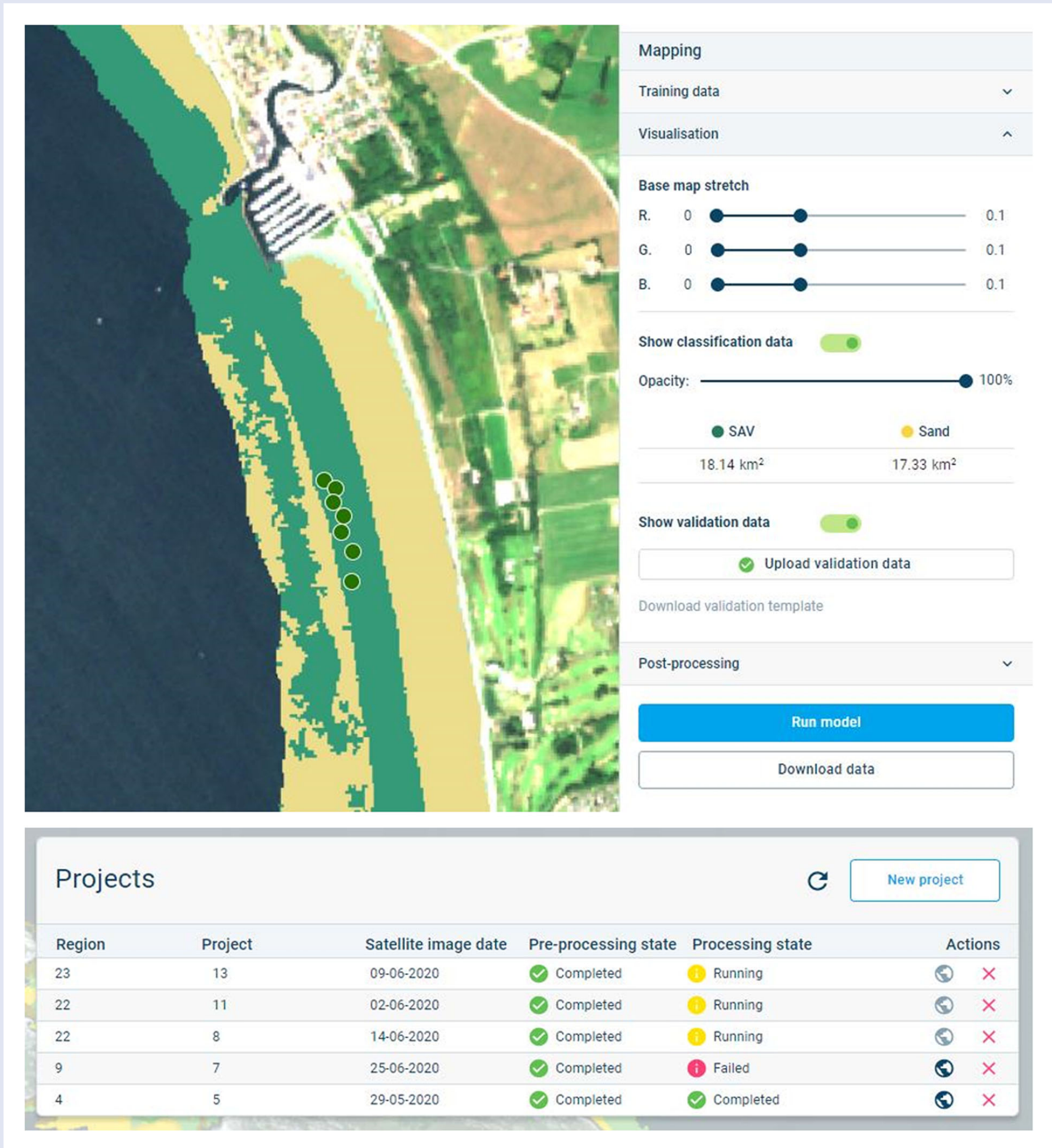

FIGURE 2 Cloud-based SAV Mapping application combining Copernicus Sentinel-2 imagery and novel machine learning techniques. Top: Visualization interface of the application; bottom: dashboard with overview of mapping project status. SAV, submerged aquatic vegetation

"references classification" (Olofsson et al., 2014) and compared both the total area and the areas overlapping with the drone classified areas to obtain estimates of "correctly" (i.e., satellite classified SAV overlapping with drone classified SAV) and "incorrectly" (i.e., satellite classified SAV found outside of drone classified SAV) classified areas. This comparison included the whole area analyzed in the drone classification also when it included areas outside the optically shallow classes described in the feasibility layer.

Cloud-based SAV mapping application

Software implementation. The whole mapping workflow from S2 image selection, preprocessing, ML model training, mapping, and visualization (as presented in the previous sections) was combined in a cloud-based, semi-automatic SAV mapping application (prototype) that enables users without experience in satellite data processing to produce their own up-to-date SAV classifications (Figure 2). The SAV mapping application uses spatial divisions encompassing

 DOI: 10.1002/ieam.4493 © 2021 The Authors

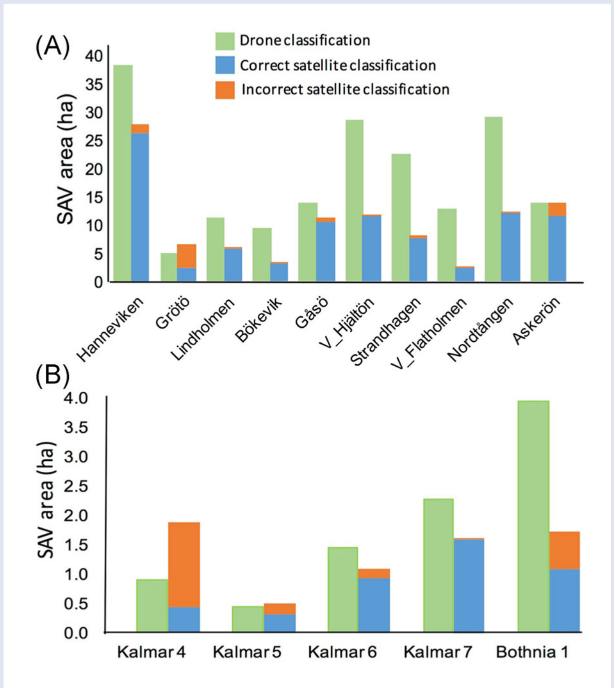

FIGURE 3 Estimated areal distribution of SAV from drone and satellite images. Classified area of submerged aquatic vegetation (SAV; ha) using drone and satellite images in (A) 10 shallow (0–6 m) soft sediment areas along the Swedish NW coast in July–August 2019, and (B) from four soft sediment areas in Kalmar Sound (Kalmar 4–7) along the SE coast, and one area in the Bothnian Bay (Bothnia 1) along the Swedish NE coast in 2020. Correct satellite classification denotes overlapping with drone classified SAV; incorrect denotes areas outside drone classified SAV. SAV, submerged aquatic vegetation

54 predefined regions (Figure 1) with the pretrained ML models as a starting point. Via a graphical user interface (GUI) in the frontend, the user is guided through the mapping workflow and, once the input image is selected and the preprocessing done, the ML model needs to be trained with new data from the area of interest to account for the conditions in the S2 image to be classified. The application allows the collection of training polygons directly on the frontend interface; alternatively, predefined polygons in standard GIS formats can be uploaded. These training polygons are stored in a database and can be accessed and modified later again. Once training samples are ready, the ML model can be run and, as soon as the classification is completed, the result is displayed on the GUI with the option of overlaying with in situ observations.

System architecture. The architecture is based on microservices and cloud services, which makes the system highly scalable and portable. The state of user projects, processing jobs, and output layers are stored in a relational database and accessible through an authenticated representational state transfer (REST) application programming interface (API). This backend communicates with the Containerized Cloud Compute API, which manages the compute jobs on the ICE Data Center Kubernetes cluster. Processing jobs, initiated on the frontend by users, independently upload their results to object storage and register them with the open-source raster layer Terracotta service, so they become available in the web interface. Both Kubernetes cluster and object storage scale easily for regular usage and handle compute and, respectively, storage in small, isolated units, such that projects do not interfere with each other and the system is very resilient to any failures. With a large number of resources available on the cluster, many tasks can be executed simultaneously. Results from the processing are stored as Cloud-optimized GeoTIFF files in ICE Data Center object storage and served to the web map via a Terracotta web map tiles API. All public interfaces are protected against unauthorized access by industry-standard authorization flows and the use of short-lived, rotating access tokens. Internal interfaces are contained in a closed network. Web connections are TLS encrypted (HTTPS).

RESULTS

Nationwide SAV map

It was feasible to map an area of 3860 km^2 of the Swedish coast with S2 imagery. In all, 1550 km^2 (41 % of total area) were mapped as SAV, 1740 (45% of total area) and 530 km^2 (14% of total area) as soft and hard substrates, respectively. This number relates to the two shallow classes delineated in the feasibility layer, for which it is feasible to see the seabed substrate in S2 imagery. From available coastal map data (sea chart), the estimated total area that is shallower than 10 m is reported to be 9300 km^2 (Naturvårdsverket, 2006). Almost all (99%) of the S2 derived data within the shallow classes of the feasibility layer is from 0 to 6.5 m deep (min 0 m, max 29.7 m, mean 0.7 m). Approximately 57% of the national water surface between 0 and 3 m deep is covered by the analysis. This is probably an underestimation of the coverage of the shallow coastline, because the coastal map data are not highly precise and tend to underestimate the depth to embrace a precautionary approach vis-à-vis maritime traffic.

Quantitative evaluation of satellite image classification accuracy

Results relative to the Swedish northwest coast. Satellite classifications of underwater vegetation in 10 shallow bays along the Swedish NW coast in 2019 exhibited relatively good accuracy of SAV in the shallow parts, particularly when using drone-generated, ground-truth points, but missed a large proportion of deeper SAV classified with drone images during the same summer. On average, 50.5% of SAV was missed in the satellite classification (range 19%–82%; Figure 3A). A comparison of the images revealed that the missed SAV was found mainly in the deeper (3–6 m) part of the bays, where the "feasibility layer" of the satellite classification excluded the deeper parts from the analyses (Figure 4). In contrast, satellite classification was accurate in classifying areas with SAV, because the percentage of

 © 2021 The Authors

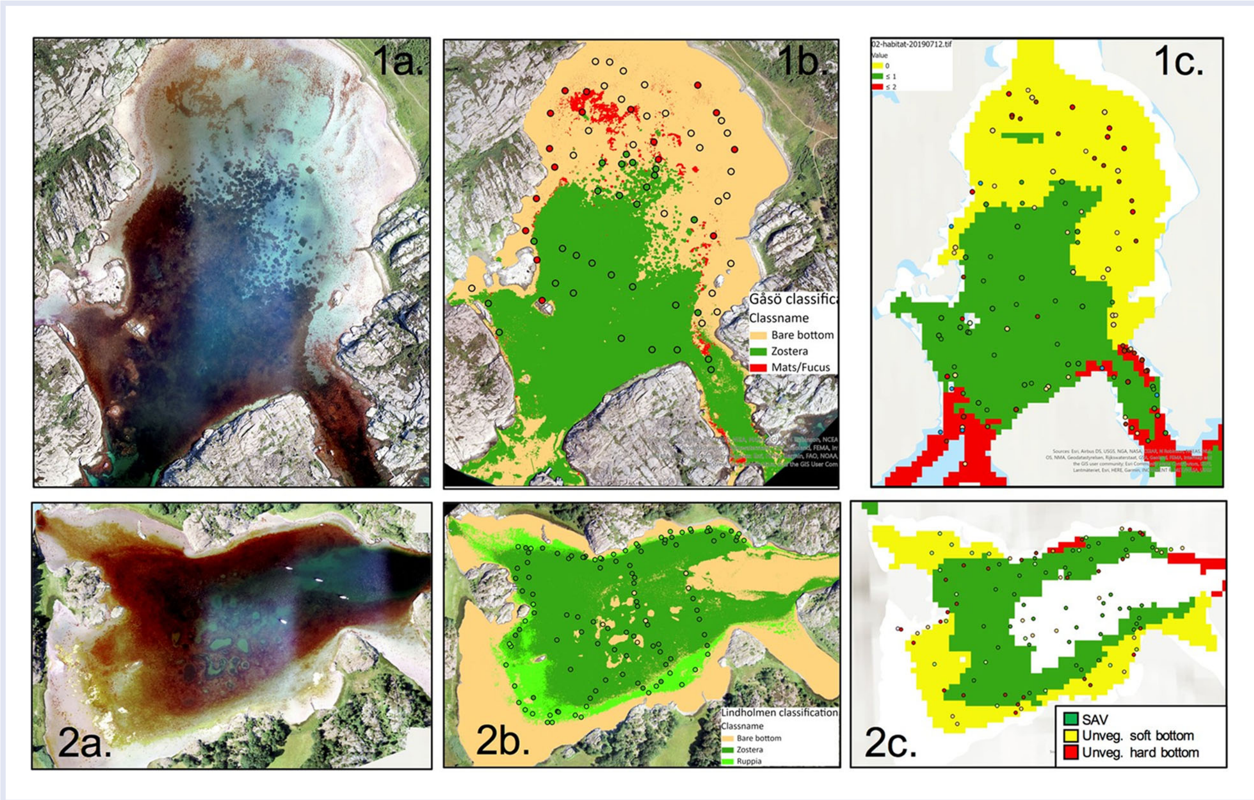

FIGURE 4 Example of classified habitats from drone and satellite images 2019 at Gåsö (1A–C) Lindholmen (2A–C) in NW Sweden. (A) Orthomosaic of drone images, (B) classified distribution of eelgrass (*Zostera*), perennial drift algae (*Fucus*), widgeon grass (*Ruppia*), and bare substrate from drone images, showing the ground-truth data as points, and (C) classified distribution of SAV, unvegetated soft and hard substrate from satellite images showing the ground-truth data as points. Please note that similar colors are used for different habitats in panel 1B and C. Note that the satellite classification of SAV at Lindholmen misses the eelgrass habitat in the deeper part of the bay because the limitation of the feasibility mask. At Gåsö, this problem was much less pronounced. SAV, submerged aquatic vegetation

incorrect classification (i.e., incorrectly classifying unvegetated substrate as SAV) was less than 6% at most sites (Figure 3A).

The accuracy estimates of satellite classifications in the feasibility layer in the shallower part of the bays, using field-based ground-truth data, revealed high user accuracy for SAV (on average 97% &; range 87%–100%); that is, it rarely classified unvegetated substrate as SAV. However, the producer accuracy was much lower (on average 47%; range 27%–68%), suggesting that it often classified SAV as unvegetated substrate. This resulted in lower total accuracy than with the drone classification (on average 49% and 86%, respectively; Figure 5A). However, using the drone classifications as ground-truth data, the total accuracy was much higher (on average 77%; range 64%–89%) and more similar to the accuracy obtained in the drone classification (Figure 5A). Thus, along the Swedish NW coast, where the water quality is relatively good and the vegetation was dominated by dense eelgrass meadows, the accuracy of the satellite classification was relatively high within the shallow part of the bay, where the feasibility layer allowed satellite classification.

Results relative to the Swedish east coast. Similar to the Swedish NW coast, the satellite classifications of four sites in Kalmar Sound along the Swedish SE coast missed most of the SAV, primarily in deeper areas outside the shallow classes of the feasibility layer. On average, 35.3% of SAV detected in the drone classification was missed in the satellite classification (range 26%–51%; Figure 3B). In addition, and in contrast to the Swedish NW coast, a large and variable proportion of SAV was incorrectly classified in the satellite image (incorrectly classifying unvegetated substrate as SAV; on average 31.2%; range 1%–77%). In the Bothnian Bay in NE Sweden, the satellite image missed a very large proportion of the SAV within the feasibility layer of the bay (72%), whereas the incorrect classification was proportionally smaller (17%; Figure 3B).

The accuracy of the satellite image within the shallow areas of the feasibility layer was relatively high in Kalmar Sound (average total accuracy of 60%), although it revealed a large variation (27%–81%) and the average user and producer accuracy for SAV were 77% and 68%, respectively. The corresponding accuracy of the drone classification for the same sites were on average 77%, 79%, and 81%, respectively (Figure 5B). The total accuracy of the satellite image within the shallow lagoon in the Bothnian Sea was also relatively high (63%) but lower than the total accuracy of the drone images (85%; Figure 5B).

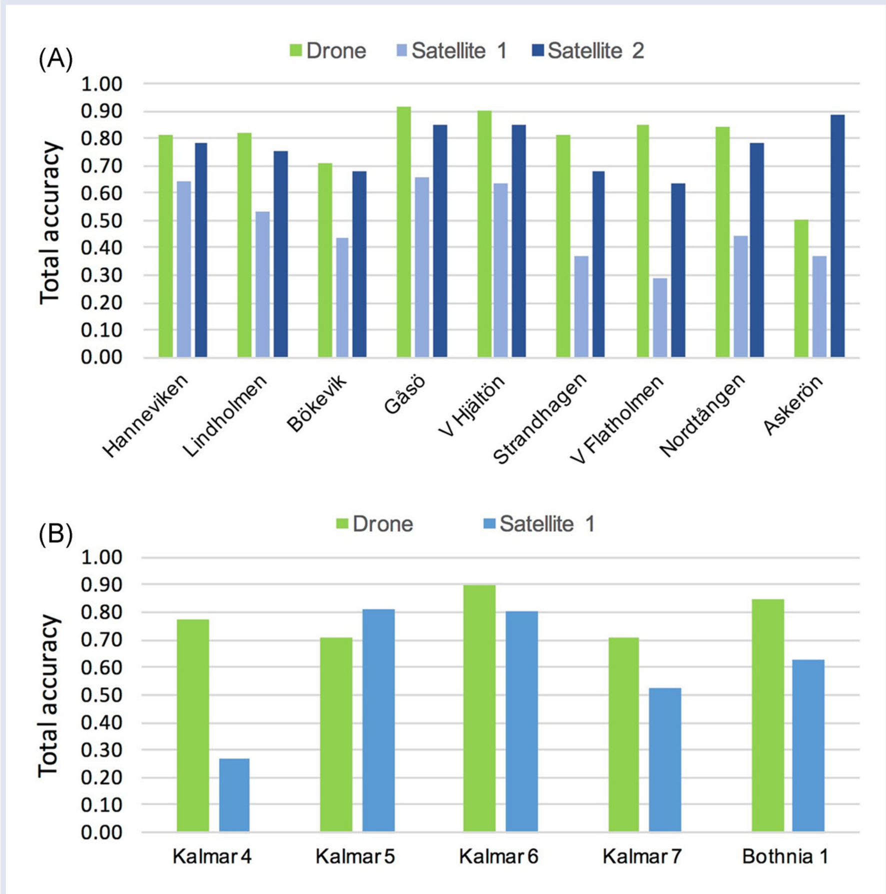

FIGURE 5 Total accuracy of classification of SAV from drone and satellite images. Estimated total accuracy from classification of SAV and unvegetated areas using drone images or satellite images in (A) nine shallow (0–6 m) soft sediment bays along the Swedish NW coast in July–August 2019, and (B) from four soft sediment areas in Kalmar Sound (Kalmar 4–7) along the SE coast, and one area in the Bothnian Bay (Bothnia 1) along the Swedish NE coast in August–September 2020. Accuracy was estimated using *ground-truth* data consisting of ca. 50–100 field points per site obtained with drop video or aqua scope (Drone and Satellite 1 estimates). Along the Swedish NW coast, an additional estimate was carried out for the satellite classification using 186–425 random points generated from drone classification as *ground-truth* data (Satellite 2), which should provide higher accuracy estimates

DISCUSSION

SAV spatial assessment

Quantitative evaluation of the accuracy of the satellite image classification showed encouraging results and identified issues with the feasibility layer used that warrant some further methodological development. Using independent field data collected with drop video and aerial drones to assess the accuracy, we found relatively high accuracy in classifying SAV in shallow soft substrate areas, particularly along the Swedish NW coast (average total accuracy 77%), where the water quality is relatively high with dense and well-defined eelgrass meadows often growing down to 5 m. For these areas, it was also relatively easy to extract good training samples for the ML model, which have contributed to the good results. Previous studies evaluating SAV in smaller areas with Sentinel-2 imagery usually report total accuracies of >80% in clear, shallow waters (Rowan & Kalacska, 2021). For areas with high water clarity and still dominant but more fragmented eelgrass growth caused by the higher wave energy (e.g., Kalmar Sound), it was more difficult to map SAV with the spatial resolution (10 m) of the S2 satellite images. This was particularly observed if a rather small area is assessed (as in the Kalmar sites) and may explain the lower total accuracy in the classification (60%) and the large proportion of unvegetated substrate incorrectly classified as Q8 SAV (on average 31%). Also here, a relatively large proportion of the deeper vegetation was missed in the satellite classification. For such areas with fragmented, patchy growth, it might be useful to introduce a "dense" and "sparse" SAV classes into the ML model to differentiate between different growth densities. Currently, the ML model assigns pixels into "hard" classes, that is, either SAV or unvegetated substrate. Mixed S2 pixels, for example, patchy or less dense SAV mixed with unvegetated areas where the underlying substrate is spectrally dominant, will be classified as unvegetated.

Most challenging was the mapping in Bothnian Bay in NE Sweden, where water clarity is substantially lower than the other areas. In turbid waters, it is harder to isolate the plant signal from the overall reflectance of the water column, because the presence of optically active material (i.e., plankton,

 © 2021 The Authors

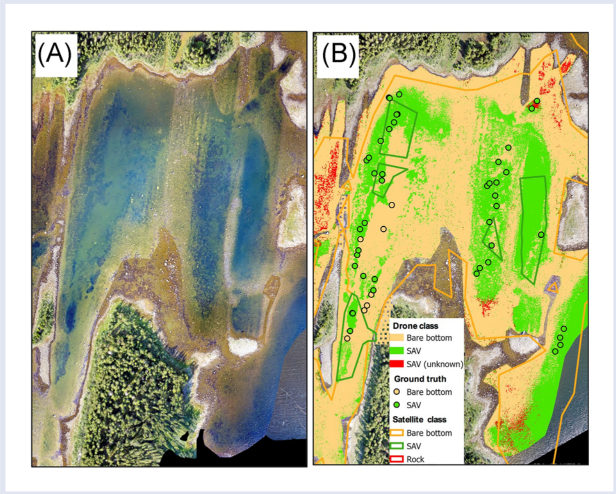

FIGURE 6 Example of classified habitats from drone and satellite images taken in 2020 at the site Bothnia 1 in the Bothnian Bay, NE Sweden. (A) Orthomosaic of drone images, and (B) classified distribution of SAV and bare substrate from drone images (filled colors) and satellite images (colored borders), showing the *ground-truth* data as points. The SAV consists of a mixture of the limnic seagrass species *Potamogeton* spp., *Vaucheria* sp. and *Myriophyllum* spp. SAV, submerged aquatic vegetation

sediment, organic molecules) affects the scattering and absorption of radiation, confounding the signals and diminishing the macrophyte contribution to the total signal measured by the satellite (Kirk, 1994; Malthus, 2017; Silva et al., 2008). The coastal waters in Bothnian Bay are brackish, and the vegetation consists of a mixture of different freshwater species with different colors, densities, and growth forms. This result in low contrast with the underlying substrate, making it difficult to both discriminate the SAV signal from the substrate in the relatively large pixel size (10 m) of the satellite imagery (Figure 6) and to define good training data for the ML model. Another issue in Bothnian Bay is the later seasonal development of the submerged vegetation communities that generally coincides with a period of lower water clarity caused by phytoplankton blooms, which again impede satellite-based mapping. In summary, such conditions are very challenging to derive coverage SAV from satellite imagery, which explains why more than 70% of the vegetation identified in the drone image was missed in the satellite classification at this site. More studies are needed to assess if this is a general problem in this region.

We mapped 1550 km^2 of SAV on the Swedish coast using S2 satellite imagery from 2019 to 2020. This is probably an underestimation because the area mapped covers mainly areas down to 2–3 m deep, and SAV detection down to the lower growth margins was not feasible with the satellite-based method (see the next section on the Feasibility layer). In a recent report, the combined seagrass and rockweed area was predicted to be 1635 km^2 for Sweden, based on data from existing literature, databases, and models (Frigstad et al., 2021). The HELCOM metadata catalog (http://metadata.helcom.fi/) estimates the seagrass area for Sweden at 4640 km^2. With the spatial resolution of S2 imagery and the method applied, it was not feasible to discriminate different species; currently, the method quantifies presence/absence of SAV. However, by integrating multitemporal S2 imagery in the workflow and capturing phenology patterns (e.g., Wolf et al., 2017), there is some potential to map different species groups if the stands are large enough and combined with information on substrate types; however, this remains to be investigated, similar to capturing population parameters such as shoot density, percentage covered, or biomass.

Potential further improvements could be achieved by training the ML model with additional training samples, specifically covering areas that did not perform well, based on in situ data, drone classifications, and local expert knowledge. However, it must be recognized that optical-based technologies using satellites alone only achieve good results in mapping SAV as long as benthic visibility is given (optically shallow waters); alternatively, other techniques should be envisaged for quantifying SAV.

Feasibility layer

The feasibility layer used in the analysis ensured that classification was only carried out at water depths in which the substrate was visible (optically shallow waters), based on the S2 imagery used for the mapping. As such, the feasibility layer sets the borders for a reliable and repeatable habitat classification. All other areas are either optically deep, owing to a range of influences, such as depth, bad visibility and/or high turbidity, benthic substrate spectrally inseparable from SAV, or frequent disturbance from ships. This limited the analysis of the shallower portions of the habitats (at depths less than approximately 3 m on the Swedish NW coast), excluding the deeper part of the SAV. Thus, the relatively high accuracy obtained in the classification is only representative for the shallow part of the bays. For the Swedish NW coast, on average, 50% of the total vegetation identified in the drone images was missed by the satellite image classification because of this restriction, resulting in severe underestimates of the available vegetation. The main limitation of using S2 for SAV mapping is that, often, the entire area to the lower depth margins of eelgrass is not captured. The depth limit is a key indicator to assess the environmental status for several international directives and defined as the deepest water depth where eelgrass grows. With drone images, we were able to map SAV in slightly deeper waters, which is related to the lower flight height (no atmospheric influence) and sensor performance (better signal-to-noise ratio) as compared with S2. Moreover, drone images are typically taken on a day with very good water conditions (high water clarity, low turbidity, calm weather conditions), which are required to achieve high overall accuracy (Nahirnick et al., 2019). To close the gap between the optically shallow areas mapped by satellites and the lower depth limits of SAV at scale, satellite-based mapping could be combined with species distribution modeling based on geophysical and environmental factors that influence eelgrass occurrence (e.g.,

 DOI: 10.1002/ieam.4493 © 2021 The Authors

Schubert et al., 2015; Staehr et al., 2019; Virtanen et al., 2018). The issues with the feasibility layer, the challenges with the patchy distribution of SAV in Kalmar Sound, and the poor water quality in Bothnian Bay are limitations that should be further explored and addressed in the development of the satellite classification method. Still, within the shallow portions of the bays included in the feasibility layer, the accuracy was relatively high and, at least for the Swedish NW coast, the estimated areal distribution of SAV was quite consistent with SAV polygons obtained from the drone classifications (e.g., Figure 4). User accuracy for SAV was on average >90%, with a small proportion of unvegetated areas incorrectly classified as SAV, resulting in a correct, but conservative, map of SAV within the shallow areas of the bays. Thus, within this shallow feasibility layer, which can be fixed between years, the semi-automatic approach to classifying SAV presented here could produce reliable estimates of SAV useful for monitoring, for example, annual changes in the areal distribution of vegetation along the coast. Many of our valuable habitats, such as lagoons, shallow bays, and mudflats, are within this feasibility layer. These shallow habitats are particularly susceptible to different anthropogenic activities, such as coastal exploitation, dredging, leisure boating, etc. (e.g., Eriander et al., 2017), and are therefore specifically important to monitor. Frequent and consistently acquired S2 imagery integrated in a semi-automatic method can thereby distinguish between chance variation and true change in SAV distribution to also detect smaller changes (<10%; Schultz et al., 2015). Other methods, such as drone-image analysis, habitat modeling, or sonar technique methods, may be more appropriate to monitoring SAV distribution along the deeper areas, in turbid waters, or in areas with a more fragmented distribution of the vegetation, and could be combined with the satellite remote-sensing approach.

CONCLUSIONS AND OUTLOOK

In this project we demonstrated the feasibility of combining Copernicus S2 imagery, novel ML techniques, and advanced data processing for large-scale, high-resolution mapping of the SAV distribution along the Swedish coast. The entire workflow was successfully integrated into the first prototype of a cloud-based, semi-automatic SAV mapping application, which makes it easy for satellite nonexperts to map SAV from up-to-date satellite observations. With this approach, a correct but conservative SAV distribution map has been derived with relatively high accuracy for clear, shallow areas (<3 m depth) and well-defined SAV stands. These shallow areas could be fixed and serve as baseline areas, where regular monitoring with up-to-date S2 imagery can reveal changes in the observed SAV distribution.

However, the project also revealed that, for vast shallow areas, turbidity obscures the signal from benthos and substrate and thereby reduces the accuracy with which S2 imagery can be applied to estimate SAV, and in particular lower depth margins, or completely prevents the satellite from seeing the seabed. This limitation could be reduced and accuracy improved by integrating complementary approaches, such as in situ observations, drone image analysis, habitat distribution modeling, or sonar techniques, for instance in the form of a hierarchical framework (Neckles et al., 2012).

The Swedish Agency for Marine and Water Management is planning to continue the development of a national method until the end of 2022, with a focus on further improving interpretation, establishing the method in all coastal counties, and enabling the monitoring of the status of shallow habitats with quantitative measures. To achieve full efficiency, the method needs to include a further step that enables monitoring and classification of environmental status. Status is the functional and legal pillar that forms the basis for reporting, assessment, and evaluation at national and international levels. Scalable and automated solutions, by combining up-to-date satellite imagery, ML, and cloud-based technology coupled with ground surveys can revolutionize environmental management and monitoring of vegetation status in shallow marine areas.

ACKNOWLEDGMENT

This work was funded by the Swedish Agency for Marine and Water Management.

CONFLICT OF INTEREST

The authors declare no conflicts of interest.

DATA AVAILABILITY STATEMENT

All of the Sentinel-2 L2A data which was used for the mapping can be freely accessed on Copernicus Open Access Hub (https://scihub.copernicus.eu/).

The mapping results are served to the portal frontend by a map tiles server, which renders the map tiles on the fly from the GeoTIFFs. This component is open source (MIT-licensed) Terracotta (https://github.com/DHI-GRAS/terracotta).

REFERENCES

Baetens, L., Desjardins, C., & Hagolle, O. (2019). Validation of Copernicus Sentinel-2 cloud masks obtained from MAJA, Sen2Cor, and FMask processors using reference cloud masks generated with a supervised active learning procedure. *Remote Sensing*, *11*(4), 433. https://doi.org/10.3390/rs11040433

Barbier, E. B., Hacker, S. D., Kennedy, C., Koch, E. W., Stier, A. C., & Silliman, B. R. (2011). The value of estuarine and coastal ecosystem services. *Ecological Monographs*, *81*(2), 169–193. https://doi.org/10.1890/10-1510.1

Cole, S. G., & Moksnes, P.-O. (2016). Valuing multiple eelgrass ecosystem services in Sweden: Fish production and uptake of carbon and nitrogen. *Frontiers in Marine Science*, *2*, 121. https://doi.org/10.3389/fmars.2015.00121

Dahlgren, T., Lindergart, M., Kilnäs, M., & Hammersland, J. (2012). *Manual för uppföljning av marina miljöer i skyddade områden. Havs- och vattenmyndigheten*. https://www.havochvatten.se/download/18.1690613b166605675de88b62/1539939098803/manual-uppfoljning-marina-miljoer-i-skyddade-omraden.pdf

DG Environment. (2017). Reporting under Article 17 of the Habitats Directive: Explanatory notes and guidelines for the period 2013–2018. Brussels.

 © 2021 The Authors

Duffy, J. E., Benedetti-Cecchi, L., Trinanes, J., Muller-Karger, F. E., Ambo-Rappe, R., Boström, C., Buschmann, A. H., Byrnes, J., Coles, R. G., Creed, J., Cullen-Unsworth, L. C., Diaz-Pulido, G., Duarte, C. M., Edgar, G. J., Fortes, M., Goni, G., Hu, C., Huang, X., Hurd, C. L., … Yaakub, S. M. (2019). Toward a coordinated global observing system for seagrasses and marine macroalgae. *Frontiers in Marine Science*, *6*, 317. https://doi.org/10.3389/fmars.2019.00317

Duffy, J. P., Pratt, L., Anderson, K., Land, P. E., & Shutler, J. D. (2018). Spatial assessment of intertidal seagrass meadows using optical imaging systems and a lightweight drone. *Estuarine, Coastal and Shelf Science*, *200*, 169–180. https://doi.org/10.1016/j.ecss.2017.11.001

Eriander, L., Laas, K., Bergström, P., Gipperth, L., & Moksnes, P.-O. (2017). The effects of small-scale coastal development on the eelgrass (*Zostera marina* L.) distribution along the Swedish west coast—Ecological impact and legal challenges. *Ocean & Coastal Management*, *148*, 182–194. https://doi.org/10.1016/j.ocecoaman.2017.08.005

European Commission. (2017). *Report from the Commission to the European Parliament and the Council—Assessing Member States' monitoring programmes under the Marine Strategy Framework Directive* (2008/56/EC). Brussels.

Ferreira, J. G., Andersen, J. H., Borja, A., Bricker, S. B., Camp, J., Cardoso da Silva, M., Garcés, E., Heiskanen, A. S., Humborg, C., Ignatiades, L., Lancelot, C., Menesguen, A., Tett, P., Hoepffner, N., & Claussen, U. (2011). Overview of eutrophication indicators to assess environmental status within the European Marine Strategy Framework Directive. *Estuarine, Coastal and Shelf Science*, *93*(2), 117–131. https://doi.org/10.1016/j.ecss.2011.03.014

Frigstad, H., Gundersen, H., Andersen, G. S., Borgersen, G., Kvile, K. O., Krause-Jensen, D., Boström, C., Bekkby, T., D'Auriac, M. A., Ruus, A., Thormar, J., Asdal, K., Hancke, K. (2021). Blue Carbon—Climate adaptation, CO2 uptake and sequestration of carbon in Nordic blue forests: Results from the Nordic Blue Carbon Project. Copenhagen.

Husson, E., Ecke, F., & Reese, H. (2016). Comparison of manual mapping and automated object-based image analysis of non-submerged aquatic vegetation from very-high-resolution UAS images. *Remote Sensing*, *8*(9), 724. https://doi.org/10.3390/rs8090724

Infantes, E., Orfila, A., Simarro, G., Terrados, J., Luhar, M., & Nepf, H. (2012). Effect of a seagrass (*Posidonia oceanica*) meadow on wave propagation. *Marine Ecology Progress Series*, *456*, 63–72. https://doi.org/10.3354/meps09754

Ke, G., Meng, Q., Finley, T., Wang, T., Chen, W., Ma, W., Ye, Q., & Liu, T.-Y. (2017). LightGBM: A highly efficient gradient boosting decision tree. 31st Conference on Neural Information Processing Systems (NIPS 2017), Long Beach, CA, USA, 3149–3157.

Kirk, J. T. O. (1994). Light and photosynthesis in aquatic ecosystems (2nd ed.). Cambridge University Press.

Kuuppo, P., Blauw, A., Møhlenberg, F., Kaas, H., Henriksen, P., Krause-Jensen, D., Ærtebjerg, G., Bäck, S., Erftemeijer, P., Gaspar, M., Carvalho, S., Heiskanen, A.-S. (2006). Nutrients and eutrophication in coastal and transitional waters. In A. G. Solimini, A. C. Cardoso, & A. S. Heiskanen (Eds.), *Indicators and methods for the ecological status assessment under the Water Framework Directive* (pp. 33–80). European Commission.

Lee, Z., Carder, K. L., Mobley, C. D., Steward, R. G., & Patch, J. S. (1999). Hyperspectral remote sensing for shallow waters: 2 deriving bottom depths and water properties by optimization. *Applied Optics*, *38*(18), 3831–3843. https://doi.org/10.1364/ao.38.003831

Main-Knorn, M., Pflug, B., Louis, J., Debaecker, V., Müller-Wilm, U., & Gascon, F. (2017). *Sen2Cor for Sentinel-2*. SPIE-Intl Soc Optical Eng. p. 3.

Malthus, T. J. (2017). Bio-optical modeling and remote sensing of aquatic macrophytes. In D. R., Mishra, I., Ogashawara, & Gitelson, A. A. (Eds), *Bio-optical modeling and remote sensing of inland waters* (pp. 263–308). Elsevier Inc.

Marbà, N., Krause-Jensen, D., Alcoverro, T., Birk, S., Pedersen, A., Neto, J. M., Orfanidis, S., Garmendia, J. M., Muxika, I., Borja, A., Dencheva, K., & Duarte, C. M. (2013). Diversity of European seagrass indicators: Patterns within and across regions. *Hydrobiologia*, *704*(1), 265–278. https://doi.org/10.1007/s10750-012-1403-7

Moksnes, P. O., Gippert, L., Eriander, L., Laas, K., Cole, S., & Infantes, E. (2016). Förvaltning och restaurering av ålgräs i Sverige—Ekologisk, juridisk och ekonomisk bakgrund.

Moksnes, P. O., Röhr, E., Holmer, M., Eklöf, J., Eriander, L., Infantes, E., & Boström, C. (2021). Major impacts and societal costs of seagrass loss on sediment carbon and nitrogen stocks. *Ecosphere*, *121*, 800. https://doi.org/10.1002/ecs2.3658

Nahirnick, N. K., Hunter, P., Costa, M., Schroeder, S., & Sharma, T. (2019). Benefits and challenges of UAS imagery for eelgrass (*Zostera marina*) mapping in small estuaries of the Canadian West Coast. *Journal of Coastal Research*, *35*(3), 673–683.

Naturvårdsverket. (2006). Sammanställning och analys av kustnära undervattensmiljö (SAKU)—Swedish Environmental Protection Agency.

Neckles, H. A., Kopp, B. S., Peterson, B. J., & Pooler, P. S. (2012). Integrating scales of seagrass monitoring to meet conservation needs. *Estuaries and Coasts*, *35*, 23–46. https://doi.org/10.1007/s12237-011-9410-x

Nielsen, S. L., Sand-Jensen, K., Borum, J., & Geertz-Hansen, O. (2002). Depth colonization of eelgrass (*Zostera marina*) and macroalgae as determined by water transparency in Danish coastal waters. *Estuaries*, *25*(5), 1025–1032. https://doi.org/10.1007/BF02691349

Olofsson, P., Foody, G. M., Herold, M., Stehman, S. V., Woodcock, C. E., & Wulder, M. A. (2014). Good practices for estimating area and assessing accuracy of land change. *Remote Sensing of the Environment*, *148*, 42–57. https://doi.org/10.1016/j.rse.2014.02.015

Rowan, G. S. L., & Kalacska, M. (2021). A review of remote sensing of submerged aquatic vegetation for non-specialists. *Remote Sensing*, *13*(4), 623. https://doi.org/10.3390/rs13040623

Schubert, P. R., Hukriede, W., Karez, R., & Reusch, T. B. H. (2015). Mapping and modeling eelgrass *Zostera marina* distribution in the western Baltic Sea. *Marine Ecology Progress Series*, *522*, 79–95. https://doi.org/10.3354/meps11133

Schultz, S. T., Kruschel, C., Bakran-Petricioli, T., & Petricioli, D. (2015). Error, power, and blind Sentinels: The statistics of seagrass monitoring. *PLoS One*, *10*(9), 1–32. https://doi.org/10.1371/journal.pone.0138378

Silva, T. S. F., Costa, M. P. F., Melack, J. M., & Novo, E. M. L. M. (2008). Remote sensing of aquatic vegetation: Theory and applications. *Environmental Monitoring and Assessment*, *140*, 131–145. https://doi.org/10.1007/s10661-007-9855-3

Staehr, P. A., Göke, C., Holbach, A. M., Krause-Jensen, D., Timmermann, K., Upadhyay, S., & Ørberg, S. B. (2019). Habitat model of eelgrass in Danish coastal waters: Development, validation and management perspectives. *Frontiers in Marine Science*, *6*, 175.

Stæhr, P. A., Groom, G. B., Krause-Jensen, D., Hansen, L. B., Huber, S., Jensen, L. Ø., Rasmussen, M. B., Upadhyay, S., & Ørberg, S. B. (2019). Use of remote sensing technologies for monitoring chlorophyll a and submerged aquatic vegetation in Danish coastal waters. Technical Report, DCE - Danish Centre for Environment and Energy No. 139.

Stumpf, R. P., Holderied, K., & Sinclair, M. (2003). Determination of water depth with high-resolution satellite imagery over variable bottom types. *Limnology and Oceanography*, *48*(1, part 2), 547–556. https://doi.org/10.4319/lo.2003.48.1_part_2.0547

SWAM. (2012). God Havsmiljö 2020 Marin strategi för Nordsjön och Östersjön Del 1: Inledande bedömning av miljötillstånd och socioekonomisk analys.

SWAM. (2014). God havsmiljö 2020 Marin strategi för Nordsjön och Östersjön Del 3: Övervakningsprogram.

TAS. (2021). *Sentinel-2 products specification document*. France.

Timmermann, K., Thomasberger, A., Hansen, L. B., Stæhr, P. A., Rasmussen, M. L., Stockmarr, A., Sengupta, S., Nielsen, L. T., & Lønborg, C. (2021). Nye overvågningsteknikker til marin vegetation. *Vand og Jord*, *28*(1), 8–11.

Torn, K., Herkül, K., Martin, G., & Oganjan, K. (2017). Assessment of quality of three marine benthic habitat types in northern Baltic Sea. *Ecological Indicators*, *73*, 772–783. https://doi.org/10.1016/j.ecolind.2016.10.037

United Nations Environment Programme. (2020). Out of the blue: The value of seagrasses to the environment and to people. Author.

Virtanen, E. A., Viitasalo, M., Lappalainen, J., & Moilanen, A. (2018). Evaluation, gap analysis, and potential expansion of the Finnish marine protected area network. *Frontiers in Marine Science*, *5*, 402.

Wikström, S. A., Carstensen, J., Blomqvist, M., & Krause-Jensen, D. (2016). Cover of coastal vegetation as an indicator of eutrophication along environmental gradients. *Marine Biology*, *163*(12), 257. https://doi.org/10.1007/s00227-016-3032-6

Wolf, P., Rößler, S., Schneider, T., & Melzer, A. (2017). Collecting in situ remote sensing reflectances of submersed macrophytes to build up a spectral library for lake monitoring. *European Journal of Remote Sensing*, *46*(1), 401–416. https://doi.org/10.5721/EuJRS20134623

 © 2021 The Authors